THE JOURNAL OF BIOLOGICAL CHEMISTRY VOL. 284, NO. 13, pp. 8898–8909, March 27, 2009

Therapeutic Ultrasound Bypasses Canonical Syndecan-4 Signaling to Activate Rac1*[S]

Received for publication, June 3, 2008, and in revised form, January 6, 2009 Published, JBC Papers in Press, January 15, 2009, DOI 10.1074/jbc.M804281200

Claire M. Mahoney[‡1], **Mark R. Morgan**[‡], **Andrew Harrison**[§], **Martin J. Humphries**[‡2], **and Mark D. Bass**[‡]

From the [‡]*Wellcome Trust Centre for Cell-Matrix Research, Faculty of Life Sciences, University of Manchester, Michael Smith Building, Oxford Road, Manchester M13 9PT, United Kingdom and* [§]*Smith and Nephew, York Science Park, Heslington, York YO10 5DF, United Kingdom*

The application of pulsed, low intensity ultrasound is emerging as a potent therapy for the treatment of complex bone fractures and tissue damage. Ultrasonic stimuli accelerate fracture healing by up to 40% and enhance tendon and ligament healing by promoting cell proliferation, migration, and matrix synthesis through an unresolved mechanism. Ultrasound treatment also induces closure of nonunion fractures, at a success rate (85% of cases) similar to that of surgical intervention (68–96%) while avoiding the complications associated with surgery. The regulation of cell adhesion necessary for wound healing depends on cooperative engagement of the extracellular matrix receptors, integrin and syndecan, as exemplified by the wound healing defects observed in syndecan- and integrin-knock-out mice. This report distinguishes the influence of ultrasound on signals downstream of the prototypic fibronectin receptors, $\alpha_5\beta_1$ integrin and syndecan-4, which cooperate to regulate Rac1 and RhoA. Ultrasonic stimulation fails to activate integrins or induce cell spreading on poor, electrostatic ligands. By contrast, ultrasound treatment overcomes the necessity of engagement or expression of syndecan-4 during the process of focal adhesion formation, which normally requires simultaneous engagement of both receptors. Ultrasound exerts an influence downstream of syndecan-4 and PKCα to specifically activate Rac1, itself a critical regulator of tissue repair, and to a lesser extent RhoA. The ability of ultrasound to bypass syndecan-4 signaling, which is known to facilitate efficient tissue repair, explains the reduction in healing times observed in ultrasound-treated patients. By substituting for one of the key axes of adhesion-dependent signaling, ultrasound therapy has considerable potential as a clinical technique.

Therapeutic approaches to the treatment of tissue wounds and bone fractures differ from the treatment of pathogen infections, tumor development, or genetic disorders. Effective wound therapy should be noninvasive, by definition, to avoid causing further tissue damage and should augment intrinsic healing processes without inducing excessive cell proliferation or extracellular matrix (ECM)[3] synthesis that lead to scarring or malformation. The advantages of accelerating repair are significant, since they not only improve patient comfort but also reduce the risk of infection following injury or surgery. A recent advance in this area has been the application of low intensity, pulsed ultrasound to a wound area, through transducers coupled to the skin via a water-based gel. The physiological benefits of this approach to bone fracture healing have been startling, with the healing times of tibial and radial fractures reduced by almost 40% (1, 2) and the maximum torque of healed femurs significantly enhanced following ultrasound treatment (3). Ultrasound is particularly beneficial for the treatment of nonunion fractures, which do not heal without intervention and are traditionally treated by surgical pinning of the bone. Ultrasound treatment results in the closure of 85% of nonunion fractures, a figure that is similar to the surgical success rate (68–96% of cases), but avoids the complications associated with surgery (4). Since 6.2 million fractures are reported annually, in the United States alone (5), ultrasound has tremendous potential as a therapeutic device. Nevertheless, since the biological mechanism of action of ultrasound is unclear, it is currently only used on a small number of patients.

Although the clinical benefits of ultrasound therapy have been established, surprisingly little is known about the cellular mechanism by which ultrasound accelerates healing. Bone repair can be conveniently divided into successive stages of inflammation, callus formation, and remodeling, and ultrasound exerts a particular influence over the inflammation and early callus formation stages, increasing deposition of ECM proteins, such as collagen and aggrecan (6). Optimization of the inflammatory response raises the possibility that ultrasound could also become a viable strategy for enhancing tissue regeneration. Although investigations into this hypothesis have not been rigorous enough to be conclusive, results from a small trial of patients with venous leg ulcers suggest that healing frequency might be improved by ultrasound (7), and in other studies, both the final tensile strength of healed rat tendons (8) and

* This work was supported by Wellcome Trust Grants 045225 and 074941 (to M. J. H.). The Bioimaging Facility microscopes used in this study were purchased with grants from the Biotechnology and Biological Sciences Research Council, Wellcome Trust, and the University of Manchester Strategic Fund. The costs of publication of this article were defrayed in part by the payment of page charges. This article must therefore be hereby marked "*advertisement*" in accordance with 18 U.S.C. Section 1734 solely to indicate this fact.

[S] The on-line version of this article (available at http://www.jbc.org) contains supplemental Fig. S1.

[1] Supported by a Biotechnology and Biological Sciences Research Council Collaborative Awards in Science and Engineering Ph.D. studentship, sponsored by Smith & Nephew UK Ltd.

[2] To whom correspondence should be addressed. Tel.: 44-161-275-5071; Fax: 44-161-275-5082; E-mail: martin.humphries@manchester.ac.uk.

[3] The abbreviations used are: ECM, extracellular matrix; MEF, mouse embryonic fibroblast; BIM, bisindolylmaleimide I; PKC, protein kinase C; PBS, phosphate-buffered saline; mW, milliwatts; RNAi, RNA interference; siRNA, small interfering RNA.

the rate of healing of rat knee ligaments (9) were improved by ultrasound treatment. The potential to augment a range of healing processes implies that the benefits of ultrasound therapy could be much broader than is currently appreciated. Ultrasound stimulation has been shown to activate a number of cellular signaling pathways, including those involving Erk (10), focal adhesion kinase (11), and vascular endothelial growth factor (12), and it culminates in enhanced ECM synthesis (6) and cell proliferation (13). However, extensive gaps in the literature covering this relatively new field make it difficult to piece together an understanding of how any of the individual signals affect cell behavior.

The processes that constitute tissue healing (proliferation, migration, differentiation, and ECM synthesis) each depend on signals activated during cell adhesion to the ECM. Cell adhesion is mediated by engagement of transmembrane ECM receptors of the integrin and syndecan families. Integrins interact with ECM molecules, such as fibronectin, through a direct protein-protein association (14), whereas syndecans bind to the polybasic regions of ECM molecules via glycosaminoglycan chains, which are covalently attached to the syndecan extracellular domain (15). There are examples of functional synergy between a number of integrin-syndecan pairs (16), and wound healing defects have been described in a number of syndecan- and integrin-knock-out mice (17–21). The most thoroughly characterized synergy exists between $\alpha_5\beta_1$ integrin and syndecan-4, and both are overexpressed on fibroblasts and endothelial cells surrounding a dermal wound (22, 23). There is extensive evidence that cooperative signaling by $\alpha_5\beta_1$ integrin and syndecan-4 is necessary for focal adhesion formation during spreading on fibronectin (24, 25), and the influence of each receptor on the small GTPases Rac1 and RhoA, which regulate membrane protrusion and cytoskeletal contraction, respectively (26, 27), has been identified as convergence points (28–30). Syndecan-4 determines GTP loading of Rac1, via PKCα (29), whereas $\alpha_5\beta_1$ integrin regulates the association of GTP-bound Rac1 with the plasma membrane, which is necessary for the activation of downstream effectors (30). Consequently, simultaneous engagement of $\alpha_5\beta_1$ integrin and syndecan-4 at the leading edge of a cell causes localized membrane protrusion and focal complex formation, resulting in directional migration toward exposed ECM that is critical for wound closure.

In the present study, we examine the effect of ultrasound on adhesion-dependent signaling and demonstrate that ultrasound can drive focal adhesion formation on a minimal integrin-binding ECM. We find that ultrasound acts by activating Rac1 and is capable of doing so in the absence of activation or expression of syndecan-4 or PKCα. The ability of ultrasound stimulation to bypass the syndecan-4 signaling axis for Rac1 regulation provides a novel insight into the mode of action of an emerging clinical therapy that warrants further investigation.

EXPERIMENTAL PROCEDURES

Antibodies and Reagents—Mouse monoclonal antibodies raised against vinculin (Sigma), Rac1, fluorescein isothiocyanate-conjugated paxillin, PKCα, PKCδ, and PKCϵ (BD Transduction Laboratories) were used according to the manufacturer's instructions. Mouse monoclonal antibody raised against active human β_1 integrin (12G10) was used as described previously (31). Rat monoclonal antibody raised against inactive human β_1 integrin (mab13) was a gift from Ken Yamada (National Institutes of Health, Bethesda, MD). Cy2- and Cy3-conjugated anti-mouse IgGs were purchased from Stratech Scientific, and Alexa Fluor680-conjugated anti-mouse IgG and TRITC-conjugated phalloidin were from Invitrogen. Recombinant fibronectin polypeptides encompassing type III repeats 6–10 (50K) and 12–15 (H/0) were expressed as recombinant polypeptides, as described previously (32), and poly-L-lysine was purchased from Sigma. The plasmid encoding the GST-PAK-1 CRIB domain was a gift from Professor Kozo Kaibuchi (Nagoya University School of Medicine, Japan).

Cell Culture—The generation of immortalized wild-type and syndecan-4$^{-/-}$ mouse embryonic fibroblasts (MEFs) has been described previously (29). To allow expression of the large T antigen, the MEFs were cultured at 33 °C in Dulbecco's modified Eagle's medium (Sigma) supplemented with 10% fetal bovine serum, 2 mM L-glutamine and 20 units/ml interferon-γ (Sigma). Primary human foreskin fibroblasts, passage number 8–25, were cultured at 37 °C in Dulbecco's modified Eagle's medium supplemented with 10% fetal bovine serum, 4.5 g/liter glucose, 1 mM sodium pyruvate, 2 mM L-glutamine, 0.1 mM non-essential amino acids, minimal essential medium vitamins, and 20 μg/ml gentamycin. 1–2 days before each experiment, cells were passaged to ensure an active proliferative state. K562 human lymphocytes were cultured in RPMI 1640 (Lonza) supplemented with 10% fetal bovine serum, 2 mM L-glutamine.

Cell Spreading and Adhesion Complex Formation Assays—For immunofluorescence, 13-mm diameter glass coverslips, placed into 6-well plates, were derivatized for 30 min with 1 mM sulfo-*m*-maleimidobenzoyl-*N*-hydrosuccinimide ester (Perbio). For spreading on mab13 monoclonal antibody, coverslips were precoated with 10 μg/ml goat anti-rat IgG Fc fragment (Stratech Scientific). For biochemical assays, 6-well tissue culture-treated plastic plates (Corning Glass) were coated directly with ligand. Coverslips or dishes were coated for 2 h at room temperature with 10 μg/ml 50K, H/0, poly-L-lysine, or mab13 in Dulbecco's PBS containing calcium and magnesium (Lonza) and blocked with 10 mg/ml heat-denatured bovine serum albumin for 30 min at room temperature (33). Equivalent ligand coating between glass and plastic was tested by enzyme-linked immunosorbent assay using the anti-fibronectin monoclonal antibody 333 (34). As described previously, cells were treated with 25 μg/ml cycloheximide (Sigma) for 2 h, to prevent *de novo* synthesis of ECM and other syndecan-4 ligands, without compromising cell migration or signaling (29, 35). Cells were detached with 0.5 mg/ml trypsin, resuspended in Dulbecco's modified Eagle's medium, 25 μg/ml cycloheximide, plated at a density of 1×10^5 cells/well, and allowed to spread at 37 °C for 2 h. Prespread cells were treated with 200 nM BIM (Calbiochem) for 30 min if appropriate and then stimulated with 10 μg/ml H/0 (40 min) or ultrasound (20 min), with or without pharmacological inhibitors, before fixing or preparing lysates. For extended time course experiments, ultrasound was only applied for the first 20 min of stimulation, in keeping with clinical ultrasound regimes, and cells were then maintained at 37 °C for the remainder of the duration, allowing the response to

develop. For immunofluorescence, cells were fixed with 4% (w/v) paraformaldehyde, permeabilized with 0.5% (w/v) Triton X-100 diluted in PBS, and blocked with 3% (w/v) bovine serum albumin in PBS. Fixed cells were stained for vinculin and actin, mounted in Prolong® Antifade (Invitrogen), and photographed on an Olympus BX51 microscope using a ×60 numerical aperture 1.40 PlanApo objective and Photometrics CoolSNAP ES camera. Images were compiled and analyzed using ImageJ software. The total area and integrated density of adhesion complexes per cell were calculated by recording the area of fluorescence intensity above an empirically determined threshold, following rolling ball background subtraction. The same threshold was used for all conditions within a single experiment.

Ultrasound Stimulation—6-well plates containing prespread MEFs were mounted onto an array of six 2.5-cm diameter ultrasound transducers (Exogen 2000; Smith and Nephew Inc., Memphis, TN), the bases of the wells coupled to the transducers using water-based gel (Exogen). The transducers generated 30 mW cm^{-2} (spatial average temporal average) pulsed ultrasound with a 1.5-MHz wave frequency, pulsed at 1 kHz for a duration of 20 min.

Flow Cytometry—For analysis of integrin activity by flow cytometry, K562 suspension cells were stimulated with ultrasound for 20 min, followed by centrifugation and resuspension in ice-cold medium. Cells were stained with primary antibody (12G10), diluted to 10 μg/ml in Dulbecco's PBS containing calcium and magnesium (Lonza), 0.02% (w/v) sodium azide on ice for 1 h. The cells were washed with PBS, 1% (v/v) fetal bovine serum, followed by 10 μg/ml secondary antibody diluted in PBS, 10% (v/v) fetal bovine serum for 30 min. For manganese stimulation, all antibodies and wash buffers were supplemented with 1 mM $MnCl_2$. Cells were then fixed with 2% (w/v) paraformaldehyde and analyzed on a Dako Cyan flow cytometer, using an excitation wavelength of 488 nm. A 530/30-nm bandpass filter was used to detect the emissions.

Rac1 Activation Assays—Active Rac1 was affinity-purified from lysates prepared in 20 mM HEPES (pH 7.4), 10% (v/v) glycerol, 140 mM NaCl, 1% (v/v) Nonidet P-40, 0.5% (w/v) sodium deoxycholate, 4 mM EGTA, 4 mM EDTA, 1 mM 4-(2-aminoethyl)-benzenesulfonyl fluoride, 50 μg/ml aprotinin, 100 μg/ml leupeptin using 300 μg of GST-PAK CRIB domain immobilized on agarose beads. Active GTPase was eluted in SDS-sample buffer, resolved by SDS-PAGE, and transferred to nitrocellulose. Transferred proteins were detected using the Odyssey Western blotting fluorescent detection system (LI-COR Biosciences UK Ltd.). This involved blocking the membranes with casein blocking buffer (Sigma) and then incubating with the anti-Rac1 primary antibody diluted 1:1000 in blocking buffer, 0.1% (v/v) Tween 20. Membranes were washed with PBS, 0.1% (v/v) Tween 20, and incubated with Alexa Fluor 680-conjugated anti-mouse IgG diluted 1:5000 in blocking buffer, 0.1% (v/v) Tween 20. After rinsing the membrane, proteins were detected using an infrared imaging system that allowed both an image of the membrane and an accurate count of bound protein to be recorded. Equivalent loading between time points was confirmed by blotting the crude lysate for vinculin. The significance of changes in Rac1 activity was established using paired Student's *t* tests of normally distributed small samples ($n = 5–10$).

RhoA Activation Assays—A commercially available Rho enzyme-linked immunosorbent assay was purchased from Tebu-bio and used according to the manufacturer's instructions. Briefly, this involved capturing GTP-RhoA from clarified cell lysate in a 96-well plate coated with the Rho-binding domain of rhotekin. Captured RhoA was then cross-linked to the plate and detected by sequential incubations with an anti-RhoA primary antibody and a horseradish peroxidase-conjugated secondary antibody. The relative amounts of bound RhoA were then measured by developing the plate with a horseradish peroxidase-sensitive dye, stopping development with dilute sulfuric acid and recording absorbance at 490 nm using a multiscan plate reader. Initial lysis steps were performed on ice and completed within 10 min to limit hydrolysis of bound GTP. Equivalent loading between time points was confirmed by total protein assay. The significance of changes in RhoA activity was established using paired Student's *t* tests of normally distributed small samples ($n = 5–10$).

Solid Phase Binding Assays—96-well plates were coated with goat anti-human γ1-Fc (1:500 dilution in PBS; Stratech Scientific) overnight at 4 °C. Washed wells were coated for 2 h at room temperature with Fc-tagged $\alpha_5\beta_1$ integrin extracellular domain, purified from CHO cell supernatant (36), before blocking for 1 h at room temperature with 10 mM Tris-Cl, pH 7.4, 150 mM NaCl, 1% (w/v) bovine serum albumin. After blocking, the plates were washed three times with 10 mM Tris-Cl, pH 7.4, 150 mM NaCl, 1 mM $CaCl_2$, 1 mM $MgCl_2$, 0.1% (w/v) bovine serum albumin and stimulated with ultrasound for 20 min, prior to a 3-h incubation with 10 μg/ml biotinylated 50K diluted in wash buffer and in the presence of 10 μg/ml 12G10 as appropriate. Bound 50K was detected using extravidin-horseradish peroxidase, diluted 1:500 in wash buffer, and the plate was developed for 30 min using 0.1% (w/v) 2,2′-azinobis(3-ethylbenzthiazoline-6-sulfonic acid) in 0.1 M sodium acetate, 0.05 M NaH_2PO_4, pH 5.0, 0.01% H_2O_2 (v/v). Absorbance readings were measured at 405 nm using an Opsys MR plate reader (Dynex Technologies).

RNAi Knockdown of PKCα—An siRNA duplex of sequence (sense) GAAGGGUUCUCGUAUGUCAUU (with ON TARGET^{TM} modification for enhanced specificity) and an siGLO®, nontargeting control duplex were purchased from Dharmacon (Thermo Fisher Scientific). 0.8 nmol of oligonucleotide was transfected into a 90% confluent 75-cm^2 flask of wild-type MEFs using Lipofectamine^{TM} 2000 reagent (Invitrogen). After 24 h, the cells were passaged and then used for experiments after a further 24 h. Expression of PKCα was tested by Western blotting.

Cell Migration—MEFs were spread on 50K-coated plates at 3×10^4 cells/well for 1.5 h before stimulation with ultrasound for 20 min or 10 μg/ml H/0. Time lapse images were captured at 10-min intervals for 12 h on a Leica AS MDW microscope using a ×5 numerical aperture 0.15 Fluotar objective and Photometrics Cascade II EM CCD camera, at 37 °C and 5% CO_2. The migration paths of all nondividing, nonclustered cells were tracked using Image J software to calculate the speed (distance/

time) and the persistence (linear displacement of a cell/total distance migrated).

RESULTS

Ultrasound Bypasses Syndecan-4 to Induce Focal Adhesion Formation—The adhesion of cells to fibronectin initiates a range of signaling cascades that result in organization of the cytoskeleton and the recruitment of molecules, including talin, vinculin, and paxillin, to integrin clusters to form focal adhesions. The formation of focal adhesions can be enhanced by the application of low intensity, pulsed ultrasound (37), which has led to the hypothesis that ultrasonic stimuli might modify or substitute for signals from ECM receptors. More incisive studies of ECM receptor function have revealed that engagement of syndecan-4, in addition to $\alpha_5\beta_1$ integrin, is necessary for focal adhesion formation on fibronectin (24, 25, 34). Therefore, we investigated whether ultrasound had a specific effect on either of these receptors or the pathways lying downstream. In order to differentiate between effects on $\alpha_5\beta_1$ integrin or syndecan-4, MEFs were assayed for the ability to spread and form focal adhesions on recombinant ligands of $\alpha_5\beta_1$ integrin and syndecan-4. To prevent the synthesis of *de novo* matrix that might compromise the interpretation of these experiments, protein synthesis was blocked by treatment with cycloheximide. As described previously (34), MEFs plated onto a recombinant 50-kDa fragment of fibronectin (50K), encompassing the binding sites for $\alpha_5\beta_1$ integrin (38), failed to form lamellipodia with vinculin or paxillin-containing focal adhesions unless stimulated with a soluble syndecan-binding fragment of fibronectin, comprising type III repeats 12–15 (H/0) (Fig. 1*B*). Stimulation of MEFs, prespread on 50K, with low intensity (30 mW cm^{-2}), pulsed ultrasound (1.5 MHz wave frequency, 1 kHz pulse frequency) for a duration of 20 min (Fig. 1*A*) resulted in the formation of lamellipodia with prominent focal adhesions that were strikingly similar to those formed in response to syndecan-4 engagement (Fig. 1*B*). The percentage of cells containing focal adhesions following stimulation with ultrasound was comparable with cells treated with H/0 and in both cases considerably higher than unstimulated cells ($p = 0.0016$ and $p = 0.0092$, respectively). The percentage of focal adhesion-positive cells was not improved further by the application of both stimuli compared with cells exposed to ultrasound or H/0 alone (Fig. 1*C*). Focal adhesion formation in response to H/0 or ultrasound was quantified further by measuring the total adhesion area per cell and revealed comparable responses to H/0 and ultrasound stimuli (Fig. 1*D* and Fig. S1*A*). Similar results were obtained from analysis of primary human fibroblasts (Fig. S1, *C* and *D*). Measurements of total integrated density of focal adhesions within a cell, which reflects the extent of vinculin clustering as well as area, also revealed no significant difference between H/0- or ultrasound-stimulated cells (Fig. 1*E*), and neither did measurements of focal adhesion length (Fig. 1*F*). These experiments demonstrate that ultrasound stimulation induces the formation of focal adhesions that are morphologically indistinguishable from those formed in response to syndecan-4 engagement by the ECM.

The ultrasound stimulus was characterized further by varying both the intensity and duration of stimulation. The relationship between ultrasound intensity and focal adhesion area followed a sigmoid curve with an inflection point of 21.4 ± 0.7 mW cm^{-2} (Fig. 1*G*). When MEFs were stimulated for varying times, a similar threshold-limited response was observed. Thus, focal adhesion area was significantly greater following 8 min of stimulation ($p = 2 \times 10^{-6}$) but not after just 6 min of stimulation ($p = 0.104$) (Fig. 1*H*). To ensure that the observed differences in adhesion contact formation were dependent on reaching a stimulus threshold rather than the time required for development of focal adhesions, MEFs were also fixed 20 min after the 2–10-min stimulation period and yielded the same result (data not shown). The concept of commitment to adhesion contact formation at a specific ultrasound threshold is consistent with *in vivo* investigations into the therapeutic benefits of ultrasound treatment, where the reductions in healing times following 30–50 mW cm^{-2} ultrasound were not improved by increasing ultrasound intensity to 100 mW cm^{-2} (39).

Having found that ultrasound stimulation could substitute for the presence of a syndecan-4 ligand to promote focal adhesion formation, we examined cells devoid of syndecan-4 expression, to assess whether ultrasound was acting on syndecan-4 itself. MEFs isolated from the syndecan-4 knock-out mouse formed focal adhesions in response to ultrasound, although, predictably, they did not respond to the soluble syndecan-4 ligand (Fig. 2*A*). Scoring cells for focal adhesion formation (Fig. 2*B*) and measurements of focal adhesion area (Fig. 2*C* and Fig. S1*B*), integrated density (Fig. 2*D*), and adhesion length (data not shown) revealed that the ultrasound-induced focal adhesions formed by syndecan-4-null MEFs were similar to those formed by wild-type MEFs. These experiments demonstrate that ultrasound acts by triggering a signal downstream of syndecan-4, thus dispensing with the contribution of one of the coupled prototypic fibronectin receptors normally required for focal adhesion formation.

The mechanism by which syndecan-4 and $\alpha_5\beta_1$ integrin cooperate during focal adhesion formation is not fully resolved, and it is possible that there is direct receptor cross-talk, whereby ligand-bound syndecan-4 activates the integrin itself. Previous investigations have shown that ultrasonic induction of molecules such as nitric-oxide synthase can be blocked by inhibiting integrins (40), which led us to test the activation state of β_1 integrin following ultrasound stimulation. Activity of β_1 integrin on the cell surface was measured by flow cytometry using a monoclonal antibody, 12G10, that specifically recognizes an activation epitope of human β_1 integrin (31). The staining of K562 lymphocytes with 12G10 could be enhanced by activating the integrin with a salt solution containing 1 mM Mn^{2+} rather than 1 mM Ca^{2+}, 0.5 mM Mg^{2+} (Fig. 3*A*). However, ultrasound stimulation had no effect on 12G10 binding in either condition (Fig. 3*A*; data not shown); nor did ultrasound improve the ability of isolated, purified integrin to bind 50K ligand in a solid phase binding assay, although driving integrin activation using 12G10 did (Fig. 3*B*). Similarly, ultrasound had no effect on integrin activity in a biological context. Integrin ligands

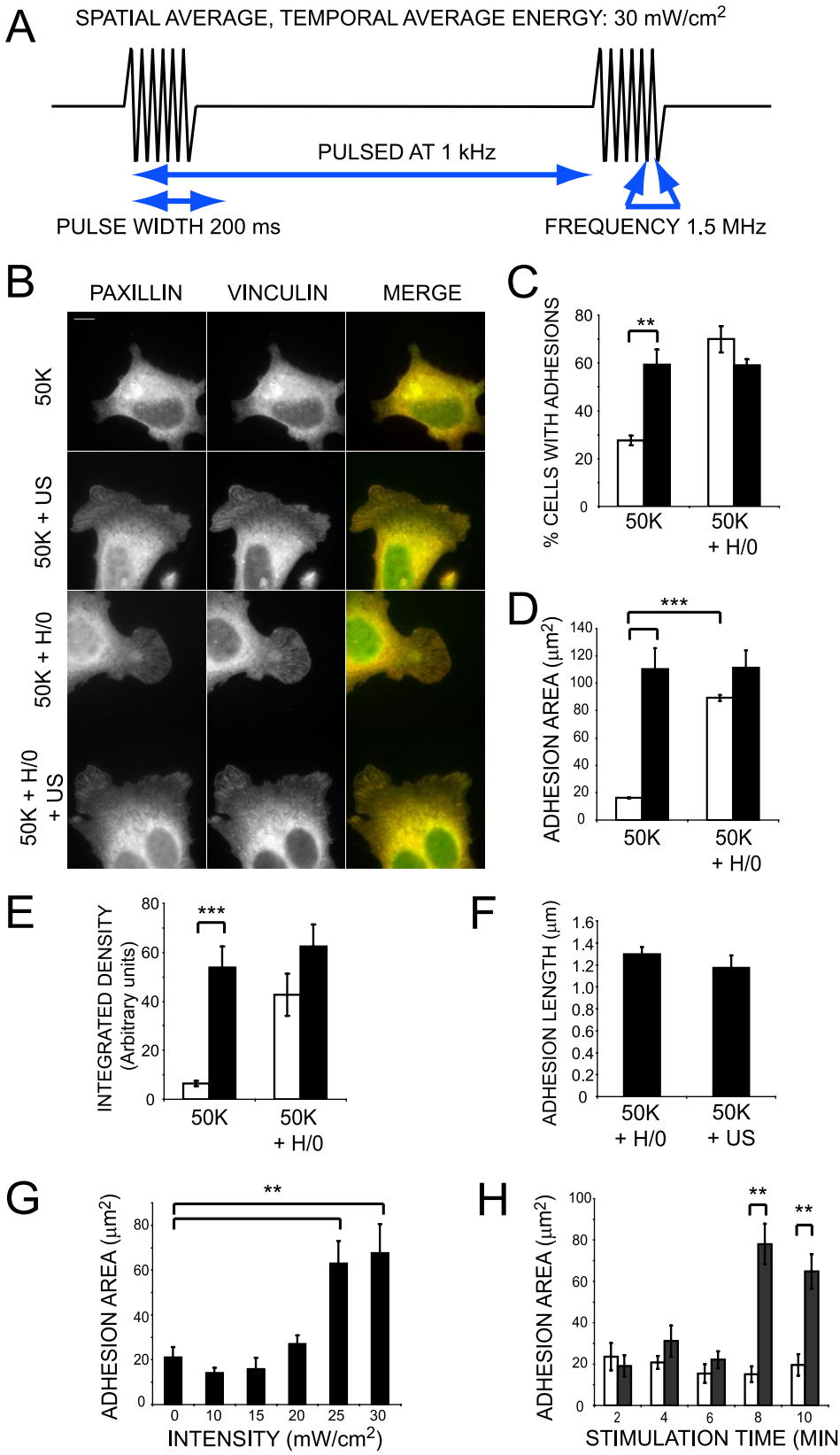

FIGURE 1. **Ultrasound stimulates focal adhesion formation independently of syndecan-4 engagement.** *A*, schematic representation of the ultrasound wave form. *B*, wild-type MEFs were spread on 50K for 2 h before stimulating with syndecan-4 ligand (H/0) for 40 min either with (*closed bars*) or without (*open bars*) ultrasound for 20 min. Fixed cells were stained for paxillin (*green*) and vinculin (*red*). *Bar*, 10 μm. *C*, 400 cells/condition were scored for focal adhesion formation. Total focal adhesion area (*D*) or total focal adhesion-integrated density (*E*) of 25–35 cells/condition was measured using image J software. *F*, average focal adhesion length of 20 cells/condition. *G*, focal adhesion area of MEFs stimulated with a range of ultrasound intensities. *H*, focal adhesion area of MEFs stimulated with ultrasound for a range of durations. *Error bars*, S.E. Significance values are as follows: *, $p < 0.05$; **, $p < 0.01$; ***, $p < 0.001$. Images and analyses are representative of experiments performed on at least three separate occasions.

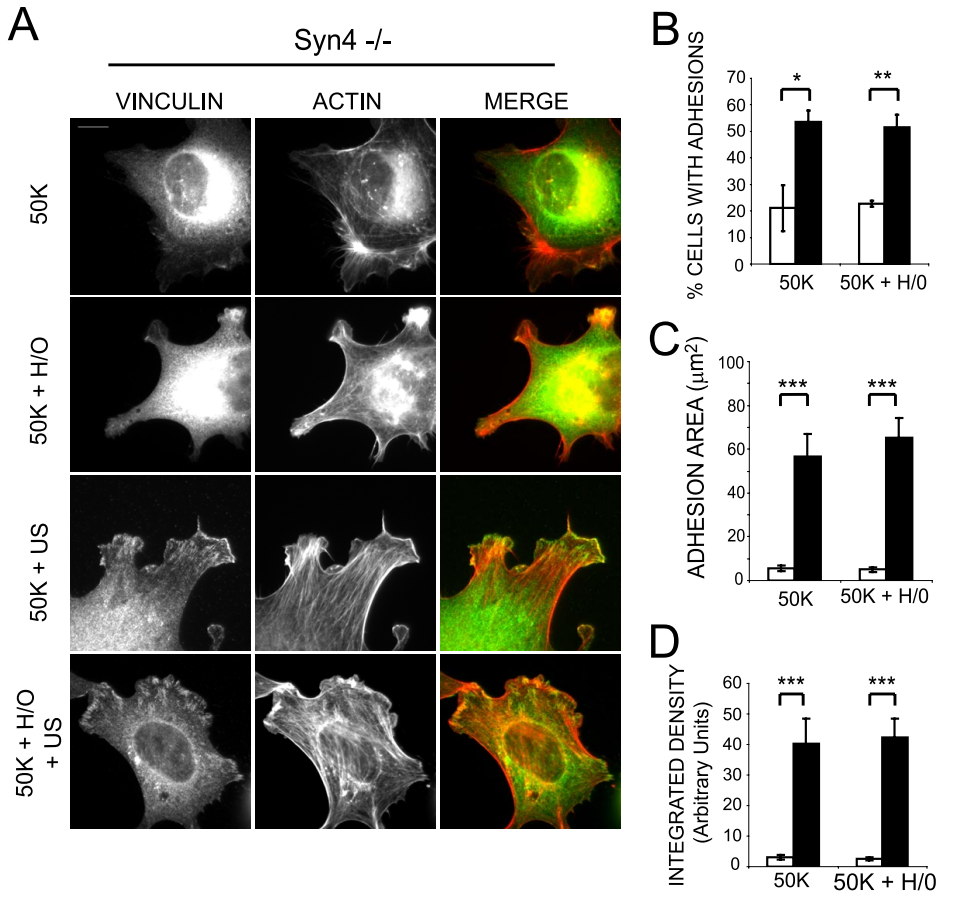

FIGURE 2. **Ultrasound stimulates focal adhesion formation independently of syndecan-4 expression.** Syndecan-4$^{-/-}$ MEFs were spread on 50K for 2 h before stimulating with syndecan-4 ligand (H/0) for 40 min either with (*closed bars*) or without (*open bars*) ultrasound for 20 min. *A*, representative cells stained for vinculin (*green*) and actin (*red*). *Bar*, 10 μm. *B*, 400 cells/condition were scored for focal adhesion formation. Total focal adhesion area (*C*) or total focal adhesion integrated density (*D*) of 25–35 syndecan-4$^{-/-}$ cells/condition was measured using image J software. *Error bars*, S.E.; significance values are as follows: *, $p < 0.05$; **, $p < 0.01$; ***, $p < 0.001$. Images and analyses are representative of experiments performed on at least three separate occasions.

are known to support cell spreading in the absence of syndecan-4 engagement, yet ultrasound did not enhance the rate of integrin-mediated spreading of MEFs on 50K (Fig. 3*C*). Furthermore, MEFs adhering to poly-L-lysine, through weak electrostatic interactions, were less well spread than those spread on fibronectin or 50K and were unaffected by ultrasound, indicating that the adhesive properties of the cell were not enhanced (Fig. 3*D*). In the absence of an integrin ligand, the syndecan-4 ligand, H/0, supported only weak cell attachment, and ultrasound stimulation was unable to substitute for signals downstream of the integrin to promote cell spreading (Fig. 3*E*). Collectively, these experiments demonstrate that, although ultrasound acts downstream of syndecan-4 to complement integrin-mediated adhesion, it does not activate the integrin directly. Finally, to test whether integrin activity was necessary for ultrasound-induced focal adhesion formation, fibroblasts were plated onto a monoclonal antibody that maintains β_1 integrin in an inactive conformation (mab13). These cells spread but failed to form focal adhesions in response to ultrasound (Fig. 3*F*), indicating that active integrin is an absolute requirement for focal adhesion formation in response to either ultrasound or syndecan-4 engagement. In summary, these experiments indicate that ultrasound acts on a signal downstream of syndecan-4, rather than $\alpha_5\beta_1$ integrin, and equally importantly that activation of both pathways is necessary for focal adhesion formation.

Ultrasound Activates Rac1—Studies *in vivo* have defined a major role for syndecan-4 in wound healing. Expression of syndecan-4 is up-regulated in fibroblasts and endothelial cells following dermal injury (23), whereas the closure of dermal wounds is retarded in the syndecan-4 knockout mouse (17). The ability of ultrasound to activate pathways downstream of syndecan-4 correlates well with the ability to reduce healing times (1, 2, 9). Syndecan-4 is understood to facilitate efficient wound closure by locally activating the small GTPase, Rac1, in response to exposed matrix (29). Active Rac1 drives membrane protrusion and the formation of nascent focal complexes and, as a consequence, causes persistent cell migration over a fibrillar matrix. To assess the effect of ultrasound stimulation on Rac1, MEFs prespread on 50K were stimulated with either H/0 or ultrasound, and active Rac1 was affinity-precipitated from lysates over a time course. Stimulation of MEFs with ultrasound or the soluble syndecan-4 ligand induced similar waves of Rac1 activity that peaked at 30 min (Fig. 4, *A* and *B*). In addition, stimulation of syndecan-4-null MEFs with ultrasound caused an enhanced wave (Fig. 4*D*), despite the cell line already having constitutively elevated levels of GTP-Rac1, in comparison with wild type MEFs (29, 41). In order to replicate the therapeutic regimes, cells were stimulated with ultrasound for a maximum of 20 min in these experiments, and then lysates were harvested after a further delay if appropriate. This approach means that there are two possible interpretations of these data, first that ultrasound triggers a wave of Rac1 activity, as detected upon engagement of syndecan-4, or second, that ultrasound causes activation of Rac1 that simply decays after removal of the stimulus. To distinguish between these possibilities, Rac1 activity was measured in cells that had been stimulated with ultrasound for the full 0–60 min and revealed a wave of activity similar to that elicited by the other treatments (Fig. 4*C*). Based on these data, it is possible to hypothesize that the therapeutic effect of ultrasound may be due to the transient activation of Rac1 that, in combination with localized inte-

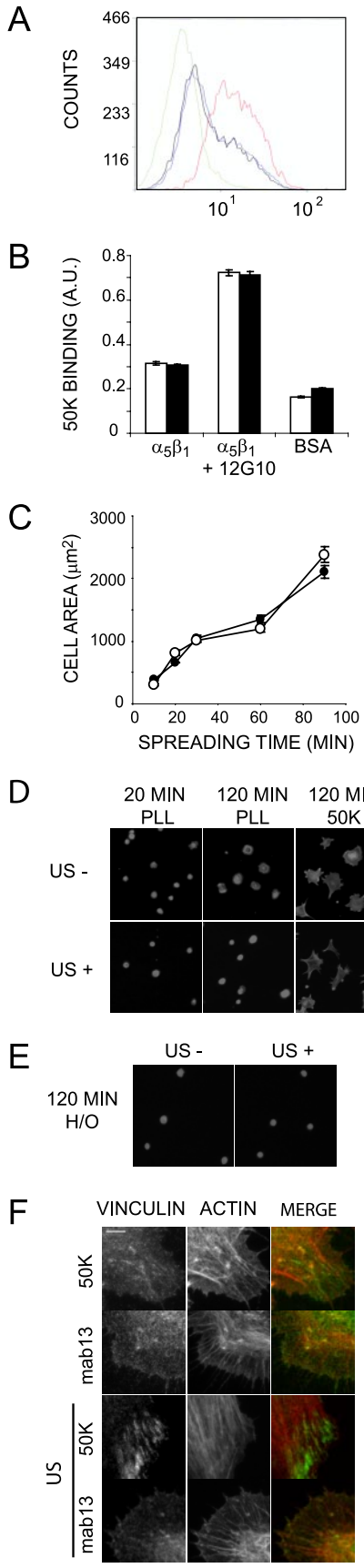

FIGURE 3. **Ultrasound does not elicit its effect through integrin activation.** *A*, flow cytometry of K562 cells following ultrasound stimulation using monoclonal antibody 12G10, which recognizes an activation epitope of human β_1 integrin. 1 mM manganese was used as a positive control to drive integrin activation. *Green*, IgG control; *black*, 12G10 with calcium/magnesium; *blue*, 12G10 with calcium/magnesium plus ultrasound; *red*, 12G10 with manganese. *B*, binding of biotinylated 50K to isolated, purified $\alpha_5\beta_1$ integrin in a solid phase assay either with (*closed bars*) or without (*open bars*) a 20-min ultrasound stimulation or the addition of the activating antibody 12G10. *C*, rate of integrin-mediated spreading of control (*open circles*) or ultrasound-stimulated (*closed circles*) MEFs. The area of 150 cells was measured using Image J software. *Error bars*, S.E. *D* and *E*, the areas of MEFs plated onto poly-L-lysine, H/0 or 50K for 120 min were unaffected by stimulation with ultrasound. *Bar*, 50 μm. *F*, fibroblasts spread on 50K or the inhibitory β_1 monoclonal antibody, mab13, and stimulated with ultrasound were stained for vinculin (*green*) and actin (*red*). *Bar*, 5 μm. *Error bars*, S.E. Each result is representative of three independent experiments.

grin engagement, would drive directional cell migration. The transient nature of Rac1 activation makes it unlikely that the efficacy of ultrasound therapy would improve with longer treatment periods, since the necessary threshold for initiation of a wave of Rac1 activity is achieved within the 20-min treatment period.

Rac1 regulation is closely coordinated with the regulation of the antagonistic GTPase, RhoA, particularly during cell spreading on fibronectin, where Rac1 activation correlates with RhoA suppression to allow membrane protrusion (42). The effect of ultrasound on Rac1 and cytoskeletal organization, coupled to the fact that RhoA has been found to be necessary for ultrasound-stimulated phagocytosis (43), led us to examine RhoA regulation in response to ultrasound. Ultrasound stimulation caused a slight, transient increase in RhoA activity (Fig. 5*A*), unlike syndecan-4 engagement, which induced suppression of RhoA activity (Fig. 5*B*) (28). The response to ultrasound was modest in comparison with stimulation with serum (42) or suppression by H/0, suggesting that RhoA is not the primary target of ultrasound action. It is notable that syndecan-4 is essential for ECM-induced Rac1 regulation (29) but is only one of the contributors toward RhoA regulation (28). This means that parallels can be drawn between syndecan-4 and ultrasound signaling pathways insofar as Rac1 appears to be a primary target of both pathways.

Ultrasound Action Is Independent of PKCα—Regulation of Rac1 by syndecan-4 is known to be mediated by PKCα (29), which is activated by direct association with the syndecan-4 cytoplasmic domain (44). The possibility that PKCα might be the target of ultrasound during Rac1 regulation was tested using siRNA knockdown and pharmacological inhibitors. Spread MEFs transfected with a nontargeting, control oligonucleotide responded to ultrasound by activating Rac1 over a similar time course to untransfected MEFs (Fig. 6*A*). Reduction of PKCα expression to less than 20% by RNAi (Fig. 6*B*), blocked syndecan-4-mediated Rac1 activation in response to H/0 (Fig. 6*D*) (29) but did not block Rac1 activation in response to ultrasound (Fig. 6*C*). In the same way, treatment of MEFs with the PKC inhibitor, 200 nM bisindolylmaleimide I (BIM), prevented H/0-induced (Fig. 6*F*) but not ultrasound-induced Rac1 activation (Fig. 6*E*), demonstrating that ultrasound exerts its influence downstream of the syndecan-4/PKCα signaling cascade. The PKCα-independent nature of ultrasound action was also manifested during focal adhesion formation. MEFs transfected with the

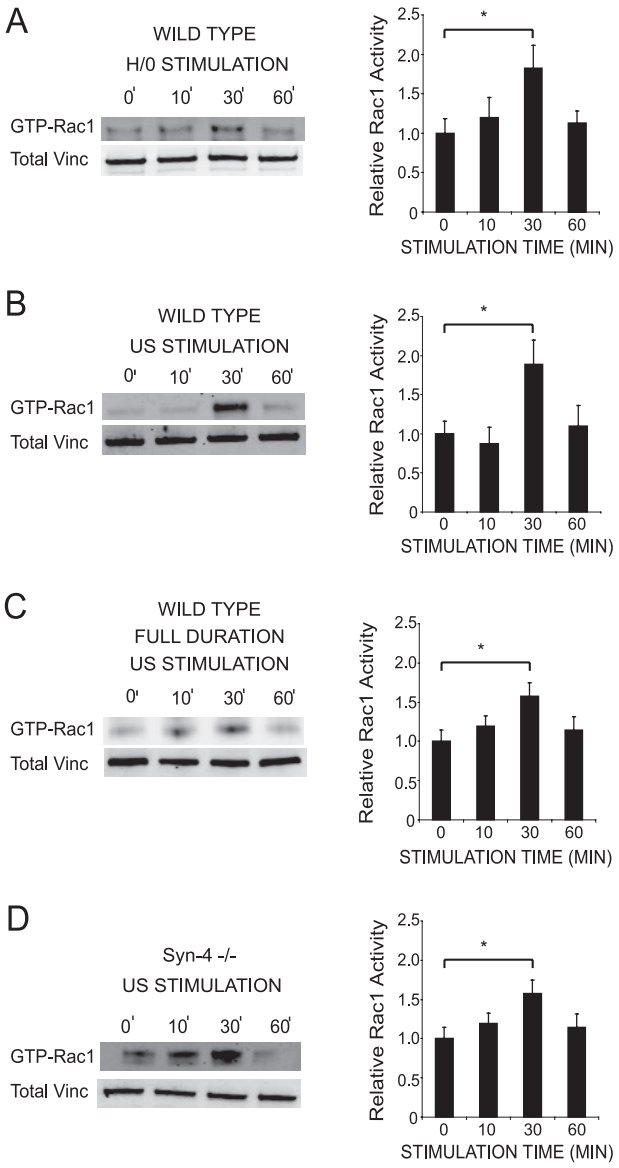

FIGURE 4. **Ultrasound causes syndecan-4-independent Rac1 regulation.** Rac1 activity was measured by effector pull-down assays in combination with quantitative Western blotting using fluorophore-conjugated antibodies. Wild-type MEFs (*A–C*) and syndecan-4-null MEFs (*D*) were prespread on 50K for 2 h and stimulated with H/0 for 0–60 min (*A*) and ultrasound for up to 20 min, followed by an appropriate delay (*B* and *D*) or by ultrasound for 0–60 min (*C*). In all cases, lysates were prepared 0–60 min after the start of stimulation. Equivalent loading between experiments was confirmed by blotting crude lysates for total vinculin. Graphs are representative of 5–10 individual experiments. *Error bars*, S.E. Significance values are as follows: *, $p < 0.05$.

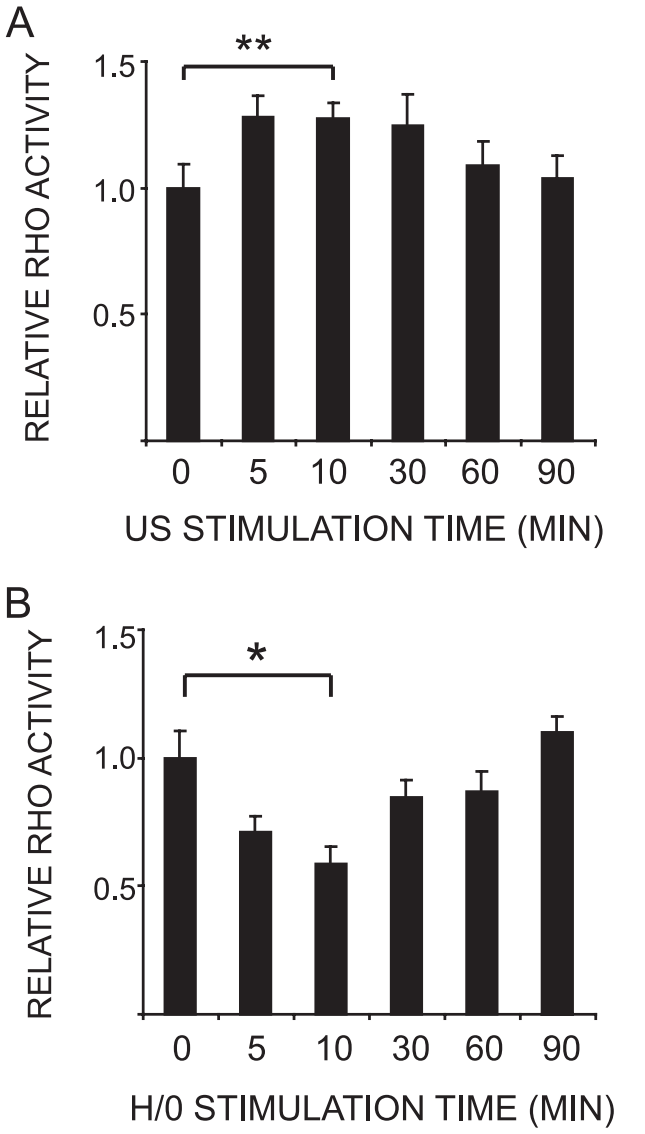

FIGURE 5. **Ultrasound stimulates a modest increase in RhoA activation.** RhoA activity was measured using a G-LISA™ RhoA activation assay. Wild-type MEFs were prespread on 50K for 2 h before stimulating with ultrasound (*A*) or H/0 (*B*) and preparing lysates over a 90-min time course. *Error bars*, S.E. Significance values are as follows: *, $p < 0.05$; **, $p < 0.01$. Graphs are representative of 12 and six individual experiments, respectively.

nontargeting control oligonucleotide responded to both H/0 and ultrasound stimuli by forming vinculin-containing focal adhesions (Fig. 7, *A*, *B*, and *D*). Reduction of PKCα expression by RNAi blocked the syndecan-4-mediated response to H/0 (Fig. 7, *B* and *C*) but did not prevent focal adhesion formation in response to ultrasound (Fig. 7, *C* and *D*). Likewise, pharmacological inhibition of PKC activity with BIM blocked focal adhesion formation in response to H/0 but not ultrasound (Fig. 7, *E–G*). Collectively, these experiments demonstrate that low intensity pulsed ultrasound can trigger the activation of Rac1 and the formation of focal adhesions through a mechanism that is independent of the syndecan-4/PKCα signaling cascade.

Ultrasound and Syndecan-4 Engagement Exert Similar Influences over Cell Migration—We have demonstrated that stimulation of cells with ultrasound or syndecan-4 ligand causes transient activation of Rac1 over similar periods. We hypothesized that the activation of Rac1 would enhance cell migration, leading to the reduction in healing times detected *in vivo* (1, 2, 9). The effect of ultrasound and syndecan-4 engagement on cell migration was tested by tracking cells plated onto 50K and then stimulated with ultrasound or H/0. The speed of cell migration was unaffected by stimulation (Fig. 8*A*). However, the persistence of cell migration was enhanced significantly ($p = 0.036$ and 0.015) in response to ultrasound and H/0, respectively (Fig. 8, *B* and *C*). The

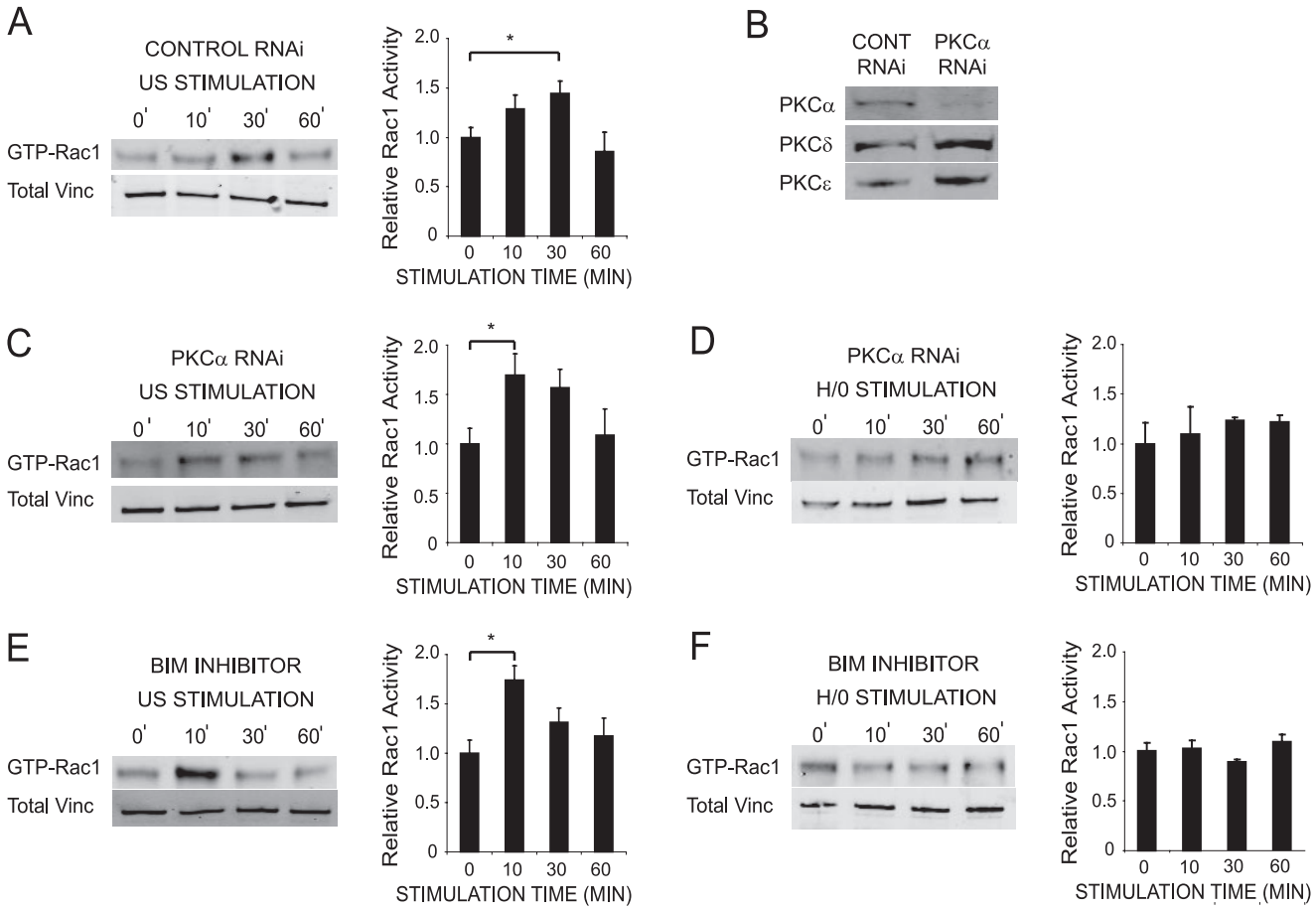

FIGURE 6. **Ultrasound-stimulated Rac1 regulation occurs independently of PKCα.** Rac1 activity was measured by effector pull-down assays in combination with quantitative Western blotting using fluorophore-conjugated antibodies. Wild-type MEFs transfected with a nontargeting control siRNA (*A*), an siRNA specific to PKCα (*C* and *D*), or treated with 200 nM BIM for 30 min before and throughout stimulation (*E* and *F*) were prespread on 50K for 2 h and stimulated with ultrasound (*A*, *C*, and *E*) or H/0 (*D* and *F*) over a 60-min time course, before preparing lysates. Equivalent loading between experiments was confirmed by blotting crude lysates for total vinculin. *Error bars*, S.E. Significance values are as follows: *, $p < 0.05$. *B*, expression levels of PKCα, PKCδ, or PKCε following RNAi. Analyses are representative of 5–10 independent experiments.

increase in persistence is consistent with earlier reports that engagement of syndecan-4 augments directionality of migration, both in cell-based assays (29) and *in vivo* (45). In this experiment, we confirm that ultrasound can indeed substitute for syndecan-4 engagement in a functional role. By overcoming the need for one of the branches of ECM-dependent signaling, particularly the branch that is specific to wound healing, ultrasound therapy represents a major step forward in clinical practice without the need to overcome the side effects that often hamper drug development.

DISCUSSION

In this study, we demonstrate that the stimulation of cells with a low intensity ultrasound device, induces a wave of Rac1 activity and focal adhesion formation and overcomes the need for syndecan-4 expression. Phylogenetic analyses have suggested that duplication of the syndecan gene in mammals occurred during the evolution of high order functions, such as wound healing (46). The model is supported by the specific wound healing defect of the syndecan-4 knock-out mouse (17), and it would be interesting to test whether the defect is overcome by treatment of the knock-out mouse with therapeutic ultrasound. It is striking that ultrasound-induced signals appear to substitute for components of a dedicated healing mechanism, rather than modifying the behavior of an integrin that is fundamental to cell survival. The connection from Rac1 signaling to wound healing is well established, and activation of Rac1 facilitates membrane protrusion and the migration of cells in culture (26, 27). Activation of Rac1 in response to ultrasound would allow the designation of a dominant lamella, which is a key step in directional cell migration (47). *In vivo*, conditional inhibition of Rac1 in the keratinocytes of transgenic mice resulted in impaired wound re-epithelialization (48), whereas expression of constitutively activated Rac1 in smooth muscle accelerated the closure of skin wounds by 2-fold (49). Consequently, the advantage of transiently activating Rac1 in patients using ultrasound is clear, and it avoids the small risks of tumor transformation that might arise if Rac1 were to be constitutively activated by pharmacological treatment (50).

The effects of ultrasound that we describe are independent of expression of syndecan-4 and PKCα, indicating that ultrasound either exerts its influence downstream of these components of the canonical syndecan-4 cascade or activates an entirely sepa-

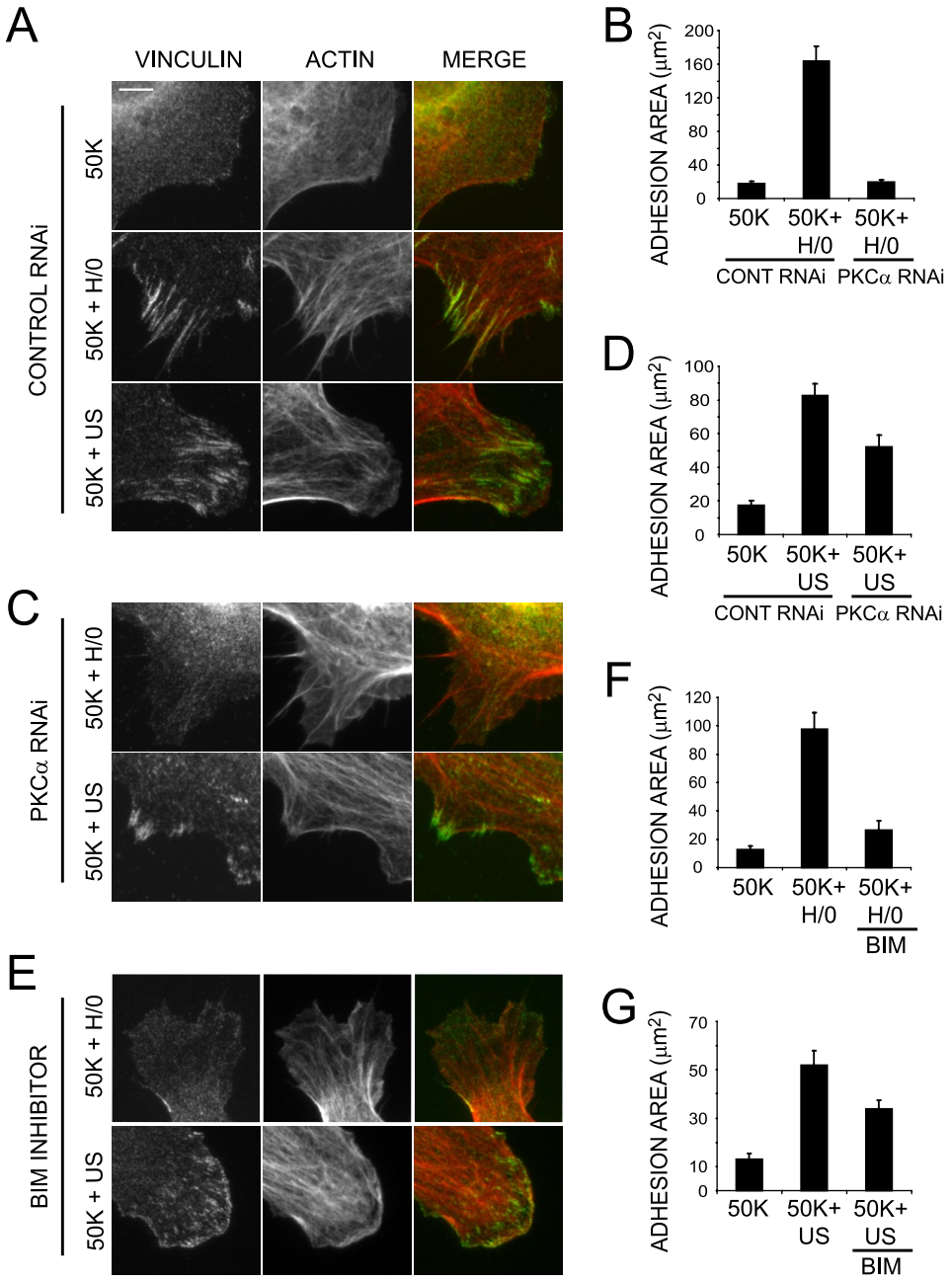

FIGURE 7. **Ultrasound-induced focal adhesion formation is independent of the syndecan-4-PKCα signaling axis.** MEFs transfected with a nontargeting control siRNA (*A*) or an siRNA specific to PKCα (*C*) or treated with 200 nM BIM throughout (*E*) were prespread on 50K for 2 h prior to stimulation with H/0 or ultrasound, followed by fixing and staining cells with vinculin (*green*) and actin (*red*). *Bar*, 5 μm. Focal adhesion area was quantified for 20 cells/condition using Image J software (*B*, *D*, *F*, and *G*). *Error bars*, S.E. RNAi and BIM results are representative of two and three independent experiments, respectively.

rate signaling cascade. The absence of RhoA suppression demonstrates that ultrasound does not recapitulate a complete adhesive response and does not target a molecule that is common to both Rac1 and RhoA regulation, downstream of syndecan-4. Gaps in our understanding of ECM receptor-dependent GTPase regulation prevent us from testing the activation of molecules downstream of PKCα, but an alternative mechanism involving force-dependent Rac1 activation in response to ultrasonic vibration is an attractive model.

Different forms of mechanical stress exert differing influences on GTPase signaling and therefore allow us to draw some conclusions about the mechanism of ultrasound action. Cytoskeletal rigidity shifts the Rac1-RhoA equilibrium in favor of RhoA, since matrix stiffness couples RhoA to its downstream effector, ROCK (51), and equibiaxial stretch inhibits Rac1 activity and lamellipodia formation (52). In the current study, we detected Rac1 activation and the formation of lamellipodial focal adhesions, and it therefore follows that ultrasound does not act by causing gross distortion of the extracellular matrix. In contrast to the stretch effect, shear flow causes the activation of Rac1 and downstream signals that include PAK and NF-κB (53). It is interesting that NF-κB activity has been found to mediate an increase in cyclooxygenase-2 expression in response to ultrasound stimulation (54), and it is possible that these previously characterized effects of ultrasound are a direct consequence of the Rac1 activation that we describe here. The similarity between the effects of ultrasound and shear flow could indicate that ultrasound acts by causing the movement of tissue fluid on a microscopic scale. The density of extracellular matrix in skin prevents rapid displacement of tissue fluid, but it is possible that vibration of the cellular milieu triggers similar signals. Whether the cell senses ultrasonic vibrations by resonation of the actin cytoskeleton remains an open question. It is difficult to determine whether disruption of the actin cytoskeleton affects ultrasound-specific signals, since cytoskeletal integrity is critical to integrin-mediated adhesion. Treatment of MEFs with pharmacological actin inhibitors, such as cytochalasin D, caused cell rounding and blocked focal adhesion formation in response to ultrasound or fibronectin stimuli (data not shown), even at low concentrations, but the fact that cytochalasin D itself influences the activities of Rac1 and RhoA (42, 55) makes such experiments difficult to interpret. Therefore, the major challenge now is to identify molecules immediately upstream of Rac1, which will complete the chain and allow us to resolve the precise mechanism of ultrasound action. Identification of the point of ultrasound action will not only allow refinement of therapeutic ultrasound routines during fracture healing and alleviate concerns over possible side effects but will

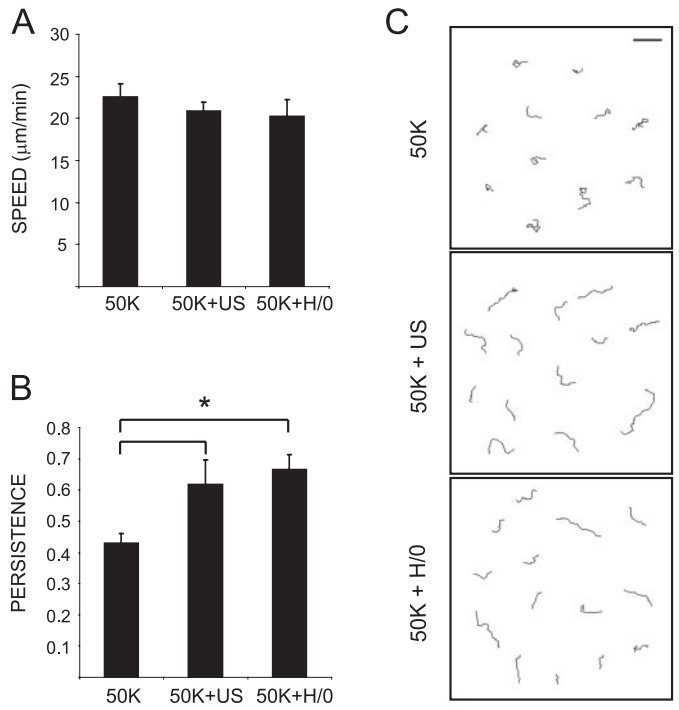

FIGURE 8. **Ultrasound and H/0 stimuli increase the persistence of cell migration.** MEFs were spread in the absence of serum on 50K for 1.5 h before the addition of H/0 or stimulation with ultrasound for 20 min. Migration was filmed for 12 h and tracked using ImageJ software. *A*, speed of migration. *B*, persistence of migration calculated by dividing linear displacement of a cell by total distance migrated. *C*, representative migration tracks. *Bar*, 200 μm. *Error bars*, S.E. of 50 different cells. *Asterisks* indicate a significant difference in persistence (*) ($p < 0.05$).

allow us to reassess the full potential of ultrasound therapy in both fracture and tissue repair.

REFERENCES

1. Heckman, J. D., Ryaby, J. P., McCabe, J., Frey, J. J., and Kilcoyne, R. F. (1994) *J. Bone Joint Surg. Am.* **76,** 26–34
2. Kristiansen, T. K., Ryaby, J. P., McCabe, J., Frey, J. J., and Roe, L. R. (1997) *J. Bone Joint Surg. Am.* **79,** 961–973
3. Azuma, Y., Ito, M., Harada, Y., Takagi, H., Ohta, T., and Jingushi, S. (2001) *J. Bone Miner. Res.* **16,** 671–680
4. Gebauer, D., Mayr, E., Orthner, E., and Ryaby, J. P. (2005) *Ultrasound Med. Biol.* **31,** 1391–1402
5. Praemer, A., Furner, S., and Rice, P. O. (1992) *Musculoskeletal conditions in the United States*, pp. 85–91, American Academy of Orthopedic Surgeons, Chicago, IL
6. Parvizi, J., Parpura, V., Greenleaf, J. F., and Bolander, M. E. (2002) *J. Orthop. Res.* **20,** 51–57
7. Al-Kurdi, D., Bell-Syer, S., and Flemming, K. (2008) *Cochrane Database Syst. Rev.* **1,** CD001180
8. Ng, C. O., Ng, G. Y., See, E. K., and Leung, M. C. (2003) *Ultrasound Med. Biol.* **29,** 1501–1506
9. Warden, S. J., Avin, K. G., Beck, E. M., DeWolf, M. E., Hagemeier, M. A., and Martin, K. M. (2006) *Am. J. Sports Med.* **34,** 1094–1102
10. Chen, Y. J., Wang, C. J., Yang, K. D., Chang, P. R., Huang, H. C., Huang, Y. T., Sun, Y. C., and Wang, F. S. (2003) *FEBS Lett.* **554,** 154–158
11. Tang, C. H., Yang, R. S., Huang, T. H., Lu, D. Y., Chuang, W. J., Huang, T. F., and Fu, W. M. (2006) *Mol. Pharmacol.* **69,** 2047–2057
12. Wang, F. S., Kuo, Y. R., Wang, C. J., Yang, K. D., Chang, P. R., Huang, Y. T., Huang, H. C., Sun, Y. C., Yang, Y. J., and Chen, Y. J. (2004) *Bone* **35,** 114–123
13. Doan, N., Reher, P., Meghji, S., and Harris, M. (1999) *J. Oral. Maxillofac. Surg.* **57,** 409–419
14. Arnaout, M. A., Mahalingam, B., and Xiong, J. P. (2005) *Annu. Rev. Cell Dev. Biol.* **21,** 381–410
15. Bernfield, M., Gotte, M., Park, P. W., Reizes, O., Fitzgerald, M. L., Lincecum, J., and Zako, M. (1999) *Annu. Rev. Biochem.* **68,** 729–777
16. Morgan, M. R., Humphries, M. J., and Bass, M. D. (2007) *Nat. Rev. Mol. Cell. Biol.* **8,** 957–969
17. Echtermeyer, F., Streit, M., Wilcox-Adelman, S., Saoncella, S., Denhez, F., Detmar, M., and Goetinck, P. (2001) *J. Clin. Invest.* **107,** R9–R14
18. Grenache, D. G., Zhang, Z., Wells, L. E., Santoro, S. A., Davidson, J. M., and Zutter, M. M. (2007) *J. Invest Dermatol.* **127,** 455–466
19. Grose, R., Hutter, C., Bloch, W., Thorey, I., Watt, F. M., Fassler, R., Brakebusch, C., and Werner, S. (2002) *Development* **129,** 2303–2315
20. Stepp, M. A., Gibson, H. E., Gala, P. H., Iglesia, D. D., Pajoohesh-Ganji, A., Pal-Ghosh, S., Brown, M., Aquino, C., Schwartz, A. M., Goldberger, O., Hinkes, M. T., and Bernfield, M. (2002) *J. Cell Sci.* **115,** 4517–4531
21. Zweers, M. C., Davidson, J. M., Pozzi, A., Hallinger, R., Janz, K., Quondamatteo, F., Leutgeb, B., Krieg, T., and Eckes, B. (2007) *J. Invest. Dermatol.* **127,** 467–478
22. Cavani, A., Zambruno, G., Marconi, A., Manca, V., Marchetti, M., and Giannetti, A. (1993) *J. Invest. Dermatol.* **101,** 600–604
23. Gallo, R., Kim, C., Kokenyesi, R., Adzick, N. S., and Bernfield, M. (1996) *J. Invest. Dermatol.* **107,** 676–683
24. Bloom, L., Ingham, K. C., and Hynes, R. O. (1999) *Mol. Biol. Cell* **10,** 1521–1536
25. Woods, A., Couchman, J. R., Johansson, S., and Hook, M. (1986) *EMBO J.* **5,** 665–670
26. Burridge, K., and Wennerberg, K. (2004) *Cell* **116,** 167–179
27. Raftopoulou, M., and Hall, A. (2004) *Dev. Biol.* **265,** 23–32
28. Bass, M. D., Morgan, M. R., Roach, K. A., Settleman, J., Goryachev, A. B., and Humphries, M. J. (2008) *J. Cell Biol.* **181,** 1013–1026
29. Bass, M. D., Roach, K. A., Morgan, M. R., Mostafavi-Pour, Z., Schoen, T., Muramatsu, T., Mayer, U., Ballestrem, C., Spatz, J. P., and Humphries, M. J. (2007) *J. Cell Biol.* **177,** 527–538
30. Del Pozo, M. A., Alderson, N. B., Kiosses, W. B., Chiang, H. H., Anderson, R. G., and Schwartz, M. A. (2004) *Science* **303,** 839–842
31. Mould, A. P., Garratt, A. N., Puzon-McLaughlin, W., Takada, Y., and Humphries, M. J. (1998) *Biochem. J.* **331,** 821–828
32. Makarem, R., Newham, P., Askari, J. A., Green, L. J., Clements, J., Edwards, M., Humphries, M. J., and Mould, A. P. (1994) *J. Biol. Chem.* **269,** 4005–4011
33. Humphries, M. J., Akiyama, S. K., Komoriya, A., Olden, K., and Yamada, K. M. (1986) *J. Cell Biol.* **103,** 2637–2647
34. Bass, M. D., Morgan, M. R., and Humphries, M. J. (2007) *Eur. Phys. J. E. Soft Matter* **3,** 372–376
35. Couchman, J. R., Hook, M., Rees, D. A., and Timpl, R. (1983) *J. Cell Biol.* **96,** 177–183
36. Coe, A. P., Askari, J. A., Kline, A. D., Robinson, M. K., Kirby, H., Stephens, P. E., and Humphries, M. J. (2001) *J. Biol. Chem.* **276,** 35854–35866
37. Zhou, S., Schmelz, A., Seufferlein, T., Li, Y., Zhao, J., and Bachem, M. G. (2004) *J. Biol. Chem.* **279,** 54463–54469
38. Danen, E. H., Aota, S., van Kraats, A. A., Yamada, K. M., Ruiter, D. J., and van Muijen, G. N. (1995) *J. Biol. Chem.* **270,** 21612–21618
39. Yang, K. H., Parvizi, J., Wang, S. J., Lewallen, D. G., Kinnick, R. R., Greenleaf, J. F., and Bolander, M. E. (1996) *J. Orthop. Res.* **14,** 802–809
40. Tang, C. H., Lu, D. Y., Tan, T. W., Fu, W. M., and Yang, R. S. (2007) *J. Biol. Chem.* **282,** 25406–25415
41. Saoncella, S., Calautti, E., Neveu, W., and Goetinck, P. F. (2004) *J. Biol. Chem.* **279,** 47172–47176
42. Ren, X. D., Kiosses, W. B., and Schwartz, M. A. (1999) *EMBO J.* **18,** 578–585
43. Zhou, S., Bachem, M. G., Seufferlein, T., Li, Y., Gross, H. J., and Schmelz, A. (2008) *Cell. Signal.* **20,** 695–704
44. Koo, B. K., Jung, Y. S., Shin, J., Han, I., Mortier, E., Zimmermann, P., Whiteford, J. R., Couchman, J. R., Oh, E. S., and Lee, W. (2006) *J. Mol. Biol.* **355,** 651–663
45. Matthews, H. K., Marchant, L., Carmona-Fontaine, C., Kuriyama, S., Larrain, J., Holt, M. R., Parsons, M., and Mayor, R. (2008) *Development* **135,** 1771–1780

46. Chakravarti, R., and Adams, J. C. (2006) *BMC Genomics* **7,** 83
47. Pankov, R., Endo, Y., Even-Ram, S., Araki, M., Clark, K., Cukierman, E., Matsumoto, K., and Yamada, K. M. (2005) *J. Cell Biol.* **170,** 793–802
48. Tscharntke, M., Pofahl, R., Chrostek-Grashoff, A., Smyth, N., Niessen, C., Niemann, C., Hartwig, B., Herzog, V., Klein, H. W., Krieg, T., Brakebusch, C., and Haase, I. (2007) *J. Cell Sci.* **120,** 1480–1490
49. Hassanain, H. H., Irshaid, F., Wisel, S., Sheridan, J., Michler, R. E., and Goldschmidt-Clermont, P. J. (2005) *Surgery* **137,** 92–101
50. Sun, D., Xu, D., and Zhang, B. (2006) *Drug Resist. Updates* **9,** 274–287
51. Bhadriraju, K., Yang, M., Alom Ruiz, S., Pirone, D., Tan, J., and Chen, C. S. (2007) *Exp. Cell Res.* **313,** 3616–3623
52. Katsumi, A., Milanini, J., Kiosses, W. B., del Pozo, M. A., Kaunas, R., Chien, S., Hahn, K. M., and Schwartz, M. A. (2002) *J. Cell Biol.* **158,** 153–164
53. Orr, A. W., Hahn, C., Blackman, B. R., and Schwartz, M. A. (2008) *Circ. Res.* **103,** 671–679
54. Hsu, H. C., Fong, Y. C., Chang, C. S., Hsu, C. J., Hsu, S. F., Lin, J. G., Fu, W. M., Yang, R. S., and Tang, C. H. (2007) *Cell. Signal.* **19,** 2317–2328
55. Price, L. S., Leng, J., Schwartz, M. A., and Bokoch, G. M. (1998) *Mol. Biol. Cell* **9,** 1863–1871